Three-State Equilibrium of *Escherichia coli* Trigger Factor

Holger Patzelt[1,2], Günter Kramer[1], Thomas Rauch[1], Hans-Joachim Schönfeld[3], Bernd Bukau[1,*] and Elke Deuerling[1,*]

[1] Zentrum für Molekulare Biologie (ZMBH), Universität Heidelberg, INF282, D-69120 Heidelberg, Germany
[2] Institut für Biochemie und Molekularbiologie, Universität Freiburg, Hermann-Herderstr. 7, D-79104 Freiburg, Germany
[3] Hoffmann-La Roche Ltd, Pharmaceutical Research, CH-4070 Basel, Switzerland

* Corresponding authors

Trigger Factor (TF) is the first chaperone that interacts with nascent chains of cytosolic proteins in *Escherichia coli*. Although its chaperone activity requires association with ribosomes, TF is present *in vivo* in a 2–3 fold molar excess over ribosomes and a fraction of it is not ribosome-associated after cell lysis. Here we show that TF follows a three-state equilibrium. Size exclusion chromatography, crosslinking and analytical ultracentrifugation revealed that uncomplexed TF dimerizes with an apparent K_d of 18 μM. Dimerization is mediated by the N-terminal ribosome binding domain and the C-terminal domain of TF, whereas the central peptidyl prolyl isomerase (PPIase) and substrate binding domain does not contribute to dimerization. Crosslinking experiments showed that TF is monomeric in its ribosome-associated state. Quantitative analysis of TF binding to ribosomes revealed a dissociation constant for the TF-ribosome complex of approximately 1.2 μM. From these data we estimate that *in vivo* most of the ribosomes are in complex with monomeric TF. Uncomplexed TF, however, is in a monomer-dimer equilibrium with approximately two thirds of TF existing in a dimeric state.
Key words: Chaperone / FKBP / PPIase / Protein folding / Ribosome.

Introduction

In the *E. coli* cytosol, Trigger Factor (TF) participates in the folding of newly synthesized proteins (Deuerling *et al.*, 1999; Teter *et al.*, 1999; Bukau *et al.*, 2000; Hartl and Hayer-Hartl, 2002). It binds to virtually all nascent polypeptides and is located on the large ribosomal subunit near the exit channel for polypeptides (Valent *et al.*, 1995; Hesterkamp *et al.*, 1996; Kramer *et al.*, 2002). It was therefore proposed that TF is the first chaperone that interacts with nascent chains and assists the co-translational folding processes.

TF has a modular structure. Its N-terminal domain mediates ribosome binding, the central PPIase domain has homology to FK506-binding proteins (FKBPs) and the C-terminal domain is of unknown function (Stoller *et al.*, 1995; Hesterkamp *et al.*, 1996, 1997). *In vitro* TF displays chaperone activity and isomerizes peptidyl-prolyl peptide bonds in chromogenic tetrapeptides and protein substrates (Stoller *et al.*, 1995; Hesterkamp *et al.*, 1996; Scholz *et al.*, 1997). Substrate binding is mediated by the central PPIase domain and independent of the presence of prolyl residues in the substrate (Scholz *et al.*, 1998; Patzelt *et al.*, 2001).

TF associates in an apparent 1:1 stoichiometry with ribosomes and this association is crucial for its interaction with nascent polypeptide chains (Hesterkamp *et al.*, 1996; Patzelt *et al.*, 2001; Kramer *et al.*, 2002). It is present in a 2–3 fold molar excess over ribosomes in the cell, suggesting an equilibrium between ribosome-associated and free forms of TF (Lill *et al.*, 1988). It is unclear whether the free form of TF is functionally important *in vivo*.

We report here a characterization of the quaternary structures of TF in its free and ribosome-associated forms.

Results

Analysis of TF's Oligomeric State by Size Exclusion Chromatography (SEC)

TF as well as the recombinant version of TF with an additional C-terminal His[6] tag elute from SEC columns within smaller volumes than expected from their molecular mass of 48 kDa (49.8 kDa for the tagged version) as computed from the primary sequence (Hesterkamp *et al.*, 1997). This prompted us to investigate the oligomeric state of TF in more detail. Since TF and the His-tagged version show identical properties regarding PPIase activity, chaperone activity and ribosome binding, we used the His-tagged protein throughout all our analysis.

We subjected purified TF to analytical SEC at room temperature using a HPLC Sec250 column. We detected only one peak at every concentration of TF tested (1–20 μM), however, the elution volumes differed depending on the protein concentration from 10.43 ml (1 μM, corresponding to approx. 70 kDa) to 9.88 ml (20 μM, corresponding to approx. 120 kDa) (Figure 1A shows a selection of concentrations). The presence of one peak at every concentration
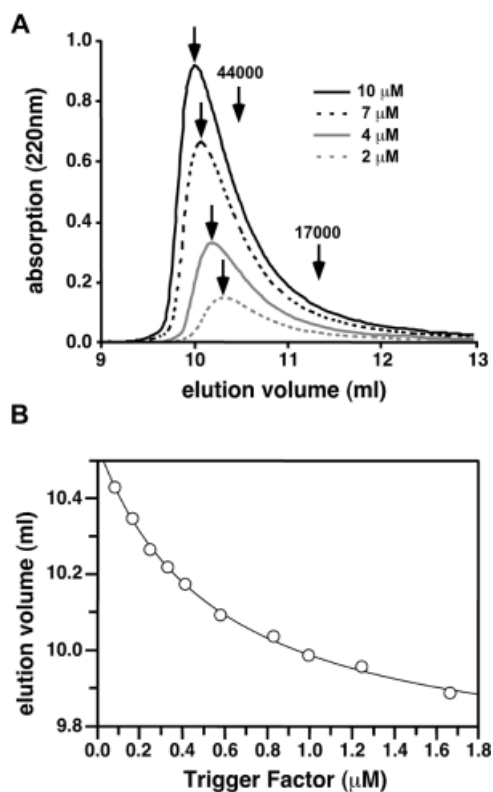
Fig. 1 Size Exclusion HPLC of TF.
(A) Elution profiles of TF at indicated concentrations using a HPLC Sec250 column. Arrows indicate the shifted peak maxima at different concentrations. Arrows with numbers represent elution volumes of molecular mass standards with indicated molecular masses. (B) Elution volumes were blotted against the estimated concentration of TF (concentration applied to the column divided by the dilution factor). Data were fitted according to the equation shown in the main text.
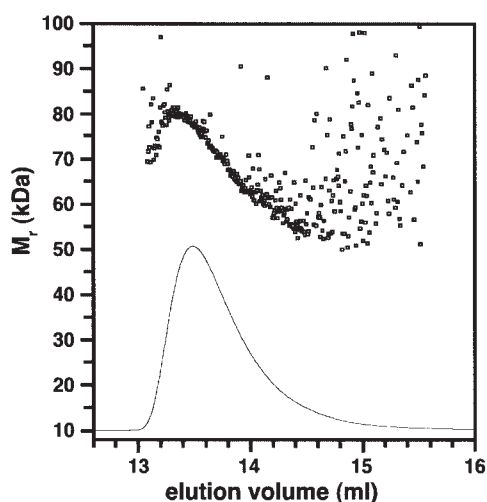

Fig. 2 Size Exclusion Chromatography and Monitoring of Absolute Molecular Mass by Static Light Scattering.
The signal from the refractive index detector from the peak region of the TF peak is given as a continuous line and the obtained molecular masses as squares. Y-axis labeling refers to molecular mass (M_r). At the peak boarders the increased scattering of molecular mass originates from non-accurate concentration determination because of a low refractive index signal.

tested is consistent with a fast equilibrium compared to the timescale of the experiment. Using a model that assumes a monomer-dimer equilibrium at every time point of the experiment, we fitted the data points (Figure 1B) as described in the literature (Richter *et al.*, 2001) according to the equation:

$$EV = EV_{mono} - (EV_{mono} - EV_{dimer}) \cdot \frac{[TF]}{[TF] + K_{d(app)}}.$$

In this equation, EV represents the measured elution volume for different TF concentrations, whereas EV_{mono} (theoretical elution volume of the monomeric species) and EV_{dimer} (theoretical elution volume of the dimeric species) as well as $K_{d(app)}$ are fitted parameters. Since TF is diluted during the experiment, we estimated the TF concentration [TF] by dividing the applied concentrations by a dilution factor. To approximate this factor, the width of the peaks at half maximal absorption, which was similar for all protein concentrations (0.6 ml), was devided by the width of the peak at the time of injection (0.05 ml) (Figure 1B). We determined a $K_{d(app)}$ of approx. 1 μM.

Size Exclusion Chromatography of TF Monitored by Static Multi-Angle Light Scattering (SEC/MALS)

For measuring absolute molecular masses of different slices of the TF peak, we next performed combined on-line differential refractive index (DRI) and MALS detection immediately after elution from a SEC Superdex200 column using an Äkta Explorer chromatography system. The average molecular mass obtained from the TF peak region was 71.0 kDa (Figure 2). Furthermore, molecular masses as obtained from subsequent slices of the TF peak were not constant, but low at the peak borders (at low protein concentration) and within the peak decreased continuously from 80 kDa at 13.2 ml to 54 kDa at 14.4 ml elution volume. This clearly indicated the presence of a mixture of monomeric and oligomeric TF species.

Determination of the TF Oligomerization State and a Dimerization Constant by Analytical Ultracentrifugation

To determine the oligomerization state of TF under equilibrium conditions we used analytical ultracentrifugation (Schonfeld and Behlke, 1998). Different oligomerization models were fitted globally to 62 sedimentation equilibrium profiles recorded at different wavelengths and at different speeds from seven different protein concentrations between 2 and 32 μM using UltraScan 5.0 software. The ideal single component model returned a molecular mass of 79.8 kDa, which is far away from 49.8 kDa as computed from the primary sequence of TF. The fits of individual scans as obtained from this model showed relatively large residuals with systematic radial dependence. However, the ideal monomer/dimer self-associating model fitted very well to the experimental data. Fits of individual profiles as obtained from this model showed
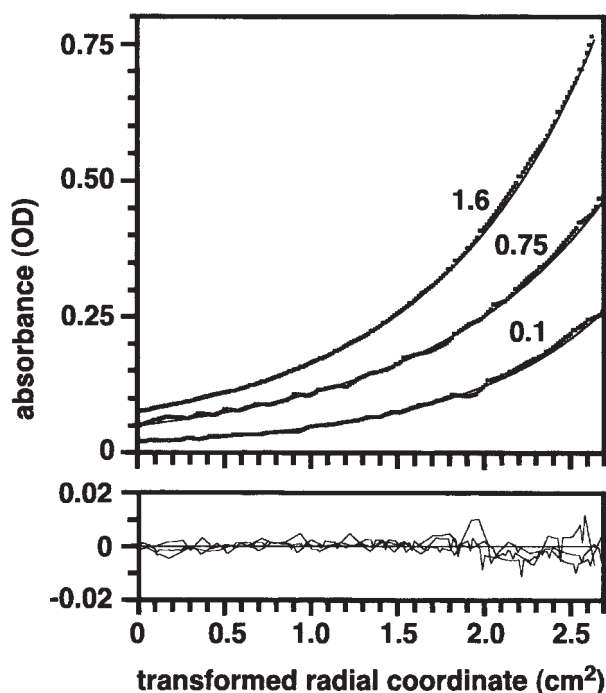
Fig. 3 Analytical Ultracentrifugation of TF.
Three out of 62 analyzed sedimentation equilibrium profiles as recorded from TF samples at 1.6, 0.75 and 0.1 mg/ml as indicated demonstrate that good fitting with the selected model was obtained throughout the complete investigated concentration range. Raw data (top, open squares) were measured at 14 000 rpm and 285 nm (1.5 and 0.75 mg/ml profiles) or 235 nm (0.1 mg/ml profile). Best fits (top, straight lines) and residuals (bottom, straight lines) are shown. For better visibility, the original OD values of the 0.75 mg/ml profile were multiplied by factor two. All fits were obtained from the global application of the ideal monomer/dimer equilibrium model and show small and equally distributed residuals.

small and randomly distributed residuals (Figure 3). The molecular mass of the monomer as returned from the global fitting process was in this case 53.4 kDa. The ideal monomer/trimer self-associating model, however, delivered again residuals with unacceptable systematic radial dependence for many profiles and a monomer molecular mass of 69.4 kDa, which is far too high. Taken together, the ideal monomer/dimer self-associating model fitted best to our experimental data and the global analysis returned a dissociation constant of 18 μM.

Glutaraldehyde Crosslinking Reveals Salt-Independent TF Dimerization

As an independent approach, we performed glutaraldehyde crosslinking to monitor TF dimer formation. We crosslinked TF at different concentrations (from 0.1 to 5 μM) with 0.1% glutaraldehyde in a buffer with physiological salt concentrations. Equal amounts of protein (5 μg) were analyzed by SDS-PAGE (Figure 4A, lanes 1 to 7). At low concentrations the majority of TF migrated as a monomeric species, whereas at high concentrations TF predominantly migrated at a molecular weight of approx-

imately 130 kDa. Depending on how the monomers are orientated to each other, crosslinking products may run with aberrant molecular masses in SDS-PAGE. We conclude that the crosslinked species of TF corresponds to the dimer described above. At high concentrations we observed minor amounts of additional TF crosslinking products with a molecular mass above 180 kDa. These adducts may correspond to higher oligomeric TF species, however, we did not detect those in size exclusion analysis and ultracentrifugation. We therefore speculate that these products represent aggregated TF species resulting from the glutaraldehyde treatment.

To investigate the contribution of ionic interactions to dimer formation, the same experiment was performed at increasing salt concentrations in the crosslinking buffer (Figure 4A, lanes 8 to 28). At all concentrations tested, the extent of TF dimer formation was similar, indicating that the dimerization predominantly involves hydrophobic interactions between the monomers.

The N- and the C-Terminal Domains of TF Contribute to Dimer Formation

We set out to evaluate which of the three TF domains (Figure 4B) contribute to dimerization. Toward this end, we performed glutaraldehyde crosslinking with his-tagged TF fragments comprising single domains (Hesterkamp *et al.*, 1997) at concentrations from 2 to 20 μM. As shown in Figure 4C, the PPIase domain [TF (145 – 247)] did not form oligomeric species (lanes 6 to 8). In contrast, the N-terminal domain [TF (1 – 144), Figure 4C, lanes 2 to 4] and the C-terminal domain [TF (248 – 432), Figure 4C, lanes 10 to 12] as well as fragments comprising two adjacent domains [TF (1 – 247) and TF (145 – 432), Figure 4C, lanes 14 to 16 and 18 to 20] formed dimers with apparent molecular masses of 38, 42, 79 and 81 kDa. For all these fragments, we also observed higher molecular weight crosslinking products at 20 μM protein concentration. As already discussed for full-length TF, this species may represent aggregates resulting from the glutardaldehyde treatment since they were not detected in size exclusion analysis (data not shown). Compared to full-length TF, a much higher protein concentration of the fragments was necessary to observe dimeric species. For the N-domain, dimerization was weak even at 20 μM protein concentration, while at that concentration dimerization of the C-terminal domain fragment was stronger (Figure 4C, compare lanes 4, 11 and 12). Interestingly, as compared to the N-domain fragment, dimerization was enhanced for the fragment TF (1 – 247) comprising the N-domain and the PPIase domain (Figure 4C, compare lanes 4 and 16). This might be explained by a conformational change in the N-domain induced by the presence of the PPIase domain. Alternatively, it may indicate that the PPIase domain contributes to dimerization when the N-domain is present. Taken together, we conclude that major contributions are made by the C-terminal domain, whereas the N-domain contributes less.
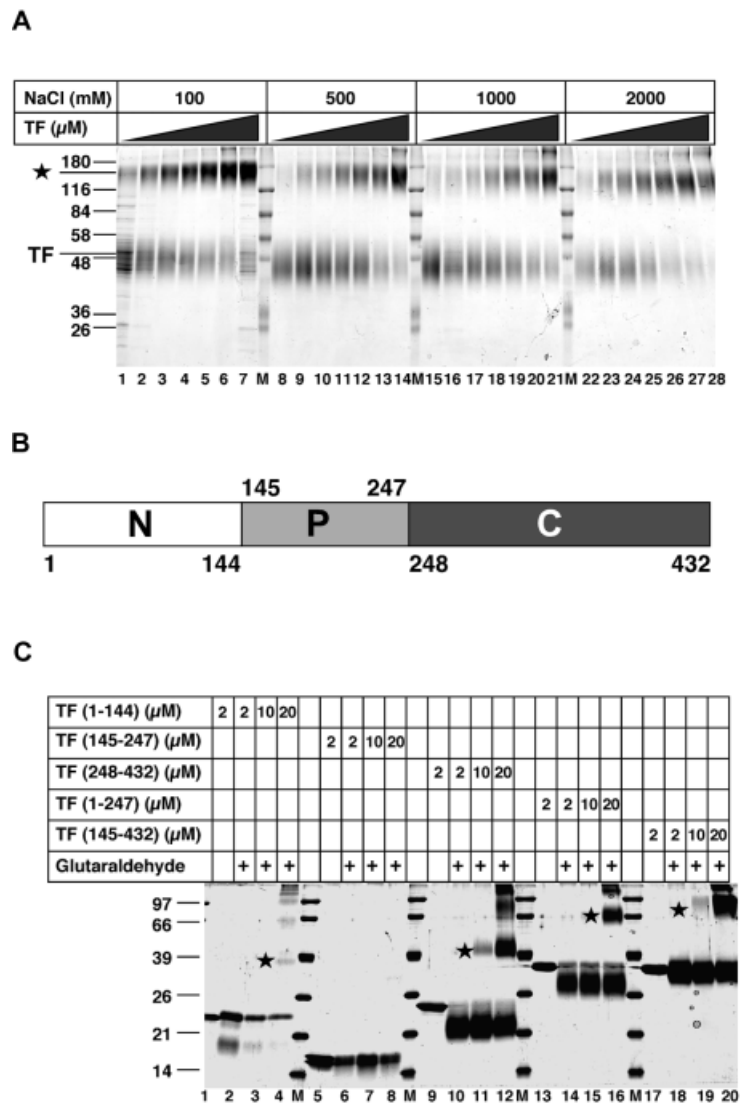
A

B

C

Fig. 4 Glutaraldehyde Crosslinking of TF and TF Fragments.
(A) Increasing concentrations of purified TF (0.1, 0.2, 0.5, 0.8, 1.0, 2.0 and 5.0 µM for every NaCl concentration) were incubated with 0.1% glutaraldehyde, followed by TCA precipitation and analysis by 10% SDS-PAGE. Equal amounts of precipitated protein were loaded in each lane (5 µg). (B) TF domain structure: N-terminal domain (N, 1–144), central PPIase domain (P, 145–247) and C-terminal domain (C, 248–432). (C) Glutaraldehyde crosslinking of TF fragments TF (1–144) (M_r = 17 300, apparent $M_{r(app)}$ on 15% SDS-PAGE = 23 000), TF (145–247) (M_r = 12 900, $M_{r(app)}$ = 16 000), TF (248–432) (M_r = 22 300, $M_{r(app)}$ = 24 000), TF (1–247) (M_r = 28 700, $M_{r(app)}$ = 35 000), TF (145–432) (M_r = 33 700 kDa, $M_{r(app)}$ = 33 000) at indicated concentrations performed as described under (A). Stars indicate the crosslinked dimers. Higher molecular mass species most probably represent aggregates resulting from the glutaraldehyde treatment since they were not detected by size exclusion chromatography. M indicates the lanes where molecular mass marker is loaded. The TF (145–247) revealed two bands in the SDS-PAGE due to the cloning procedure creating a second start codon of the gene (gene products differ by four additional N-terminal amino acid residues but show similar properties regarding PPIase activity).

We further analyzed whether the N- and C-terminal domains formed mixed oligomers using all possible fragment combinations as well as mixtures of full length TF with TF fragments. Unfortunately, these crosslinking products could not be analyzed since the crosslinked bands were broad and migrated at similar positions in the SDS-PAGE as the oligomeric species observed in Figures 4A and 4C (data not shown). Moreover, with this experiment, it would not be possible to distingiush between oligomeric species resulting from domain contacts within the dimer or within the monomer itself.

To investigate the contributions of the N- and the C-terminal domain, we used a more specific crosslinking approach. Since TF does not contain cysteine residues, we exchanged residue K46 to cysteine by site-directed mutagenesis and coupled the purified mutant protein to the photoinducible crosslinker BPIA (TF-K46C-BPIA) *via* the cysteine. K46 was chosen because it is located in a conserved region within the N-domain and is predicted to be within an exposed loop structure (Kramer *et al.*, 2002). We did not engineer the C-terminal domain since it is only poorly conserved among TF proteins and mutagenesis cannot be directed.

Incubation of 2 µM TF-K46C-BPIA at 30 °C to equilibri-

A

	1	2	3	4	5	6	7	8	9	10	11	12	13	14
TF-K46C-BPIA	+	+	+	+	+	+	+	+						
TF (1-432)		+							+					
TF (1-144)				+						+				
TF (1-247)					+						+			
TF (145-247)						+						+		
TF (145-432)							+						+	
TF (248-432)								+						+
UV-light		+	+	+	+	+	+	+	+	+	+	+	+	+

★ [97 —
66 —
TF —
39 —
26 —
21 —
14 —

1 2 3 4 5 6 7 8 9 10 11 12 13 14

B

			S	P	S	P	S	P
TF-K46C-BPIA					+		+	
Ribosomes			+				+	
UV-light			+		+		+	
Fraction			S	P	S	P	S	P

★ [97 —
66 —
TF — ☆
39 —
26 —
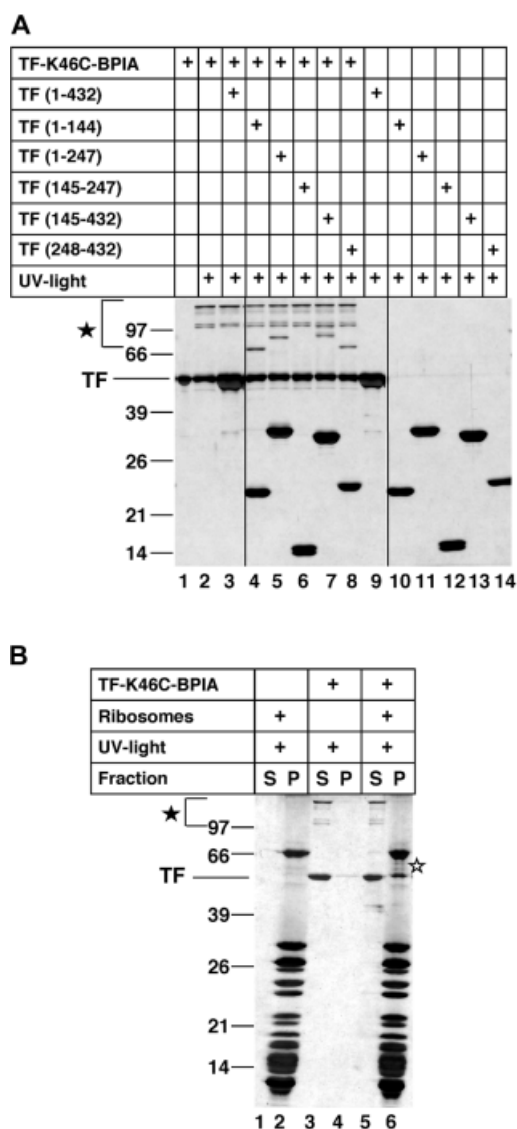21 —
14 —

1 2 3 4 5 6

Fig. 5 Specific Crosslinking of Soluble and Ribosome-Associated TF.
(A) Two μM TF-K46C-BPIA was incubated with 8 μM of TF-fragments where indicated and crosslinked by UV exposure. Subsequently, samples were analyzed by SDS-PAGE and silver staining. (B) Four μM TF-K46C-BPIA was incubated with 2 μM purified ribosomes and crosslinked by UV light. By sucrose cushion centrifugation soluble TF was separated from ribosome bound species and analysed by SDS-PAGE and silver staining. Filled stars and brackets indicate the crosslinked dimers. Open star indicates TF crosslinks to ribosomal proteins.

um and subsequent UV exposure led to the appearance of at least three distinct higher molecular mass bands in the SDS-PAGE (Figure 5A, compare lanes 1 and 2). The double band at approx. 98 kDa corresponds to TF dimers. The more prominent band at approx. 130 kDa could represent a crosslinked TF dimer migrating with aberrant size. Addition of 8 μM TF (145–247) did not result in additional crosslinking products (Figure 5A, lane 6). This is consistent with the above finding that the PPI-ase domain does not significantly contribute to dimeriza-

tion. In contrast, addition of fragments [TF (1–144), TF (1–247), TF (145–432) and TF (248–432)] containing the N- and/or the C-terminal domain revealed additional crosslinking products (Figure 5A, lanes 4, 5, 7, 8). According to their apparent sizes (76, 80, 81 and 74 kDa as judged by SDS-PAGE) these products correspond to mixed oligomers between TF-K46C-BPIA and the fragments. Since the crosslinker BPIA has a length of only 10 Å, these data suggest that, firstly, in the TF dimer, the N- and the C-terminal domains of one monomer are in close vicinity to the N-domain of the other. Secondly, the N- and the C-terminal domains of one subunit are in close vicinity to each other.

TF Monomers Associate with Ribosomes

To elucidate the oligomeric status of TF in association with the ribosome, we incubated 4 μM TF-K46C-BPIA with 2 μM purified ribosomes isolated from TF deficient cells. After UV crosslinking soluble TF was separated from ribosome bound TF by sucrose cushion centrifugation. Interestingly, we found the dimeric crosslinking products described above exclusively in the supernatant, whereas the ribosomal pellet fraction did not contain products corresponding to oligomeric TF (Figure 5B, compare lanes 3 and 5 with 6). Ribosome-associated TF crosslinked only to ribosomal proteins but not to another TF molecule (Kramer *et al.*, 2002). We conclude that TF is bound in a monomeric state to ribosomes.

For quantitative analysis, we investigated rebinding of increasing amounts of TF (0.5 to 20 μM) to 2 μM of purified ribosomes (Figure 6A). In the substoichiometric range TF was mainly found in the ribosomal pellet. At 4 μM TF (2:1 TF to ribosomes) ribosomes were apparently saturated with TF and concentrations above 4 μM did not significantly increase the amount of TF bound to ribosomes. Quantification of the ribosome bound TF and subsequent data fitting by a quadratic equation using the GraFit program (Version 5.0.1) led to an apparent K_d for the TF-ribosome complex of approximately 1.2 μM (Figure 6B).

Discussion

We have shown here that TF exists in a three-state equilibrium. In association with the ribosome TF is monomeric, whereas in its uncomplexed state TF is distributed in a monomer/dimer equilibrium.

Analysis of TF oligomers was performed by SEC, light scattering and analytical ultracentrifugation. SEC was used for first estimation of TF´s molecular size. HPLC analysis revealed one peak for different TF concentrations, however, the elution volume varied concentration dependently. The phenomenon can be explained by a fast equilibrium between monomeric and oligomeric TF. The observed peak maxima corresponded to molecular masses of 70 kDa for low TF concentrations (monomeric TF) and of 120 kDa for high TF concentrations
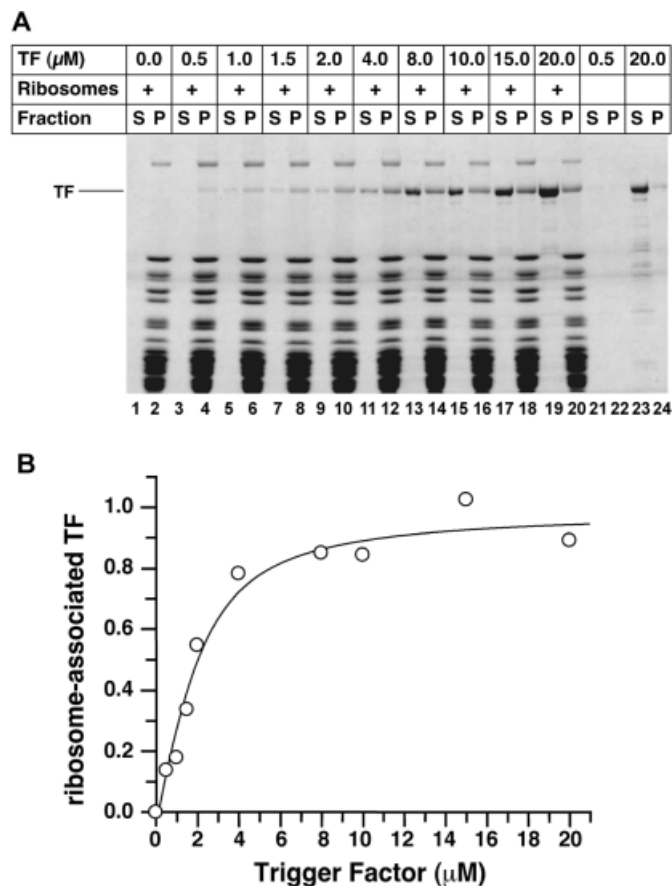
Fig. 6   Rebinding of TF to Ribosomes.
(A) Two μM of purified ribosomes were incubated with indicated amounts of purified TF and ribosome-bound TF was isolated as described in the Legend to Figure 5, panel (B). (B) Ribosome-bound TF was quantified using MacBAS and data were fitted according to a quadratic equation using the GraFit program, Version 5.0.1.

(oligomeric TF). Both values are above the theoretical molecular masses of 49.8 and 99.6 kDa, respectively. In general, the molecular masses determined by SEC may be too high or too low, dependent on whether the structure of the protein under investigation is more elongated than that of the reference proteins or whether the protein interacts with the column support in an unspecific manner (Schonfeld and Behlke, 1998). Independent of molecular shape and possible column interactions, the molecular mass of TF was measured by size exclusion chromatography and on-line static light scattering. Absolute masses from 54 to 80 kDa were obtained from different slices of the TF peak, indicating a reversible monomer/oligomer equilibrium.

Assuming a monomer/dimer equilibrium, we estimated an apparent TF dimerization constant from the size exclusion HPLC experiments, similar to a recent study with Hsp90 (Richter *et al.*, 2001). For Hsp90 the authors showed that the chaperone elutes as a single peak in size exclusion HPLC analysis with concentration dependent elution times. For Hsp90 as well as for TF, the dynamics of the monomer-dimer transition are too fast to observe both species simultaneously in gel fitration. In contrast to Hsp90, elution profiles of TF were asymmetric, indicating

partial separation of the monomeric and dimeric species, which is not taken into account by the equation used. Therefore this estimated dimerization constant may be inaccurate.

More accurately, we determined the K_d value by analytical ultracentrifugation. This method allows to observe TF dimerization under equilibrium conditions. We found that TF dimerizes with a dissociation constant of approximately 18 μM. Since analytical ultracentrifugation is the benchmark method for accurate molecular mass determinations, we consider this K_d value as more reliable than the value obtained by size exclusion HPLC analysis.

By two independent crosslinking approaches we further investigated TF dimer formation. Firstly, we used glutaraldehyde as an unspecific crosslinking agent that covalently links amine groups of lysyl residues. Secondly, the UV-activatable crosslinker BPIA with a 10 Å spacer was attached to the N-domain of TF. Glutaraldehyde crosslinking experiments provide evidence for contacts of TF domains, whereas the BPIA crosslinking approach monitors which domains of one TF monomer are in close vicinity to the N-terminal domain of the other. Dimeric species were observed for full-length TF in both approaches. Glutaraldehyde crosslinking further revealed
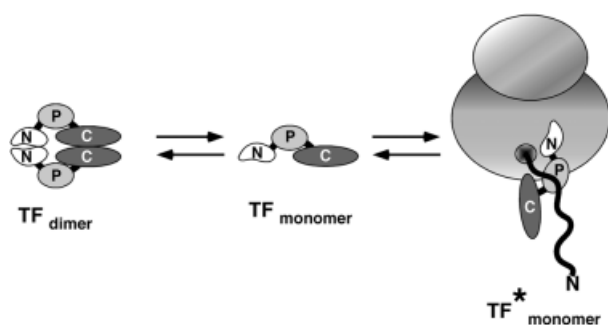
Fig. 7 Model of TF´s Three-State Equilibrium.
TF is monomeric when associated with the ribosome (TF*$_{monomer}$).
The asterisk indicates that the TF conformation might differ from
the conformation of non-ribosome associated TF$_{monomer}$. In solu-
tion, TF follows a monomer-dimer equilibrium (TF$_{monomer}$, TF$_{dimer}$).

contacts between N- and C-terminal domains, respec-
tively. Interestingly, the C-terminal domain or the frag-
ment TF (145 – 432) including this domain showed dimer
formation at much lower concentrations as compared to
the N-terminal domain or TF (1 – 247). This indicates that
the C-terminal domain plays a major role in dimerization.
Moreover, BPIA crosslinking showed that the N-terminal
domain of one monomer is in close vicinity to the N-ter-
minal and the C-terminal domain of the second
monomer. Throughout this analysis, the PPIase domain
itself never yielded a crosslinking product. However, con-
clusions from crosslinking experiments are limited due to
the specificity and positioning of the crosslinking agent,
which may cause false negative results. Therefore, we
cannot completely exclude a contribution of the PPIase
domain to dimer formation although we consider it as un-
likely. This conclusion is supported by the finding that for
other dimeric members of the FKBP-family, dimerization
also does not involve the PPIase domain but is mediated
by flanking domains (Ramm and Pluckthun, 2001). Taken
together, our data are consistent with a head-to-head ori-
entation of the monomer subunits within the dimers (Fig-
ure 7).

Interestingly, we found that TF in its ribosome-associ-
ated state is strictly monomeric. This hypothesis was
confirmed by the finding that crosslinked dimers of TF-
K46C-BPIA were exclusively present in the supernatant
fraction but never in the ribosomal pellet. Alternatively,
this might be caused by structural rearrangements of the
TF coupled crosslinker resulting in an orientation where
the BPIA cannot crosslink to the second monomer. We
consider this possibility as unlikely since TF binds to ri-
bosomes with a 1:1 stoichiometry even when present in
10-fold excess over ribosomes. We determined a disso-
ciation constant for the TF-ribosome complex of approx-
imately 1.2 μM.

Using this value and the K_d of 18 μM for dimer forma-
tion and assuming the physiological concentrations of TF
(50 μM; Teter *et al.*, 1999) and ribosomes (20 μM; Lill *et al.*,
1988), we estimate that approximately 39% of TF form

dimers, 26% are present as a monomer and 35% are as-
sociated as monomers with ribosomes. Furthermore, ap-
prox. 90% of the ribosomes contain TF. This estimation is
rather crude since it does not include any substrate inter-
action in all three TF states nor different ribosomal states
(*e.g.* translating and non-translating) where TF associa-
tion may be modified.

We assume that the TF three state equilibrium is of
physiological relevance. Firstly, monomeric and dimeric
TF may have different cellular functions. Secondly,
dimers may represent a storage form ensuring saturation
of ribosomes with TF. In this context it is interesting to
note that the engineered cysteine residue C46, which we
used for BPIA-crosslinking of TF molecules, is also capa-
ble of crosslinking TF to ribosomes. Moreover, during pu-
rification procedure, we observed cleavage of TF at this
position (Kramer *et al.*, 2002). It therefore seems plausible
that the ribosome binding site in TF is masked by dimer
formation and thus protected from protease cleavage.

Materials and Methods

Mutant Construction and Protein Purification

The TF-K46C mutation was created using the QuikChange site-
directed mutagenesis kit from Stratagene and the plasmid
pDS56-*tig*-his$_6$ (Hesterkamp *et al.*, 1997) as template according
to the manufacturer's instructions. Sequence integrity of the
construct was verified by DNA sequencing. TF, TF-fragments
and TF-K46C (all proteins carrying six His residues at the C-ter-
minus) were purified *via* Ni/NTA agarose and anion exchange
chromatography and checked for structural integrity by CD
spectrometry and PPIase activity as described (Hesterkamp
et al., 1997; Zarnt *et al.*, 1997). Protein concentrations were de-
termined using Bradford (Bio-Rad) and bovine serum albumin as
a standard and checked additionally by SDS-PAGE.

Size Exclusion HPLC Analysis and Data Evaluation

Size exclusion HPLC was performed with a flow rate of 1 ml/min
on a BioCAD SPRINT system (Applied Biosystems) with a
Sec250 column (Applied Biosystems, molecular mass range:
10 – 600 kDa) in 20 mM Tris, pH 7.5, 100 mM NaCl, 1 mM EDTA.
The column was equilibrated over night and calibrated using the
gel filtration standard from Bio-Rad (catalog #151-1901). The TF
concentrations applied to the column were varied between 1 μM
and 20 μM. Data were fitted using the GraFit program, Version
5.0.1.

Size Exclusion Chromatography Monitored by Static Light Scattering (SEC/LS)

A Superdex 200 column (HR10/30; Amersham Pharmacia, Upp-
sala, Sweden) with an optimal separation range of 10 – 600 kDa
and an exclusion volume of 7.4 ml was equilibrated with 20 mM
Tris-HCl pH 7.5, 100 mM NaCl, 1 mM EDTA at 0.5 ml/min using an
Äkta Explorer chromatography system (Amersham Pharmacia).
The size exclusion column was connected in-line with a LS de-
tector (mini DAWN Tristar; Wyatt Technology, Santa Barbara,
USA) and a refractive index detector (Shodex RI-74; Showa
Denko, Kawasaki, Japan). Fifty μl of TF at a concentration of
about 3.2 mg/ml (64 μM) were injected into the column. Molecu-
lar masses were computed by the ASTRA software (version

4.73.04; Wyatt Technology). ASTRA computes the molecular mass *via* the basic light-scattering equation by using the intensity of the scattered light and the protein concentration. Protein concentration was computed from the refractive index detector signal and assuming a refractive index increment of 0.180 ml/g as a general value for proteins. Because of the small molecular size of TF (hydrodynamic radius is far below 10 nm) no significant angular dependence of the scattering was observed (Wen *et al.*, 1996).

Analytical Ultracentrifugation

Recombinant TF from the anion exchange chromatography purification step was extensively dialyzed against 20 mM Tris-HCl pH 7.5, 100 mM NaCl, 1 mM EDTA and then diluted to 1.6, 1.3, 1.0, 0.75, 0.5, 0.25 and 0.1 mg/ml using the same buffer. 110 µl of each dilution were transferred to the sample compartments of one of seven double-sector cells. The reference sectors of the cells were filled with 130 µl of dilution buffer. The cells were positioned in a eight-hole rotor and centrifugation in an Optima XL-A analytical ultracentrifuge was performed at 20 °C. Immediately after reaching a speed of 3000 rpm, wavelength scans of each cell from 200 to 400 nm were taken at a fixed position within the liquid column. From these spectra optimal wavelengths λ were selected for subsequent radial scans (280, 285 and 275 nm for 1.6 – 0.75 mg/ml, 280, 285 and 240 nm for 0.5 mg/ml, 280, 240 and 235 nm for 0.25 mg/ml and 280, 235 and 230 nm for 0.1 mg/ml). The speed was increased to 10 000 rpm. After one day equilibria were achieved and radial scans of the concentration gradients at all above wavelengths were automatically performed. Similarly radial scans were taken after reaching equilibria at 14 000 rpm and at 18 000 rpm.

A buffer density of ρ = 1.0035 g/cm^3 was measured and a partial specific volume of $\bar{v}$ = 0.736 cm^3/g was computed from the TF primary sequence. Data analysis was performed using the linux version of the UltraScan 5.0 software (Borries Demeler, www.ultrascan.uthscsa.edu). The extinction coefficient profile was fitted from the wavelength scans obtained at 3000 rpm and the molar extinction coefficient of 17 442 M^{-1}cm^{-1} at 280 nm, as calculated from the TF primary sequence, and then used for internal conversion of optical into molar concentration units.

Glutaraldehyde Crosslinking Experiments

TF concentrations from 0.1 – 10 µM and TF fragment concentrations from 2 to 20 µM were incubated for 15 min at 30 °C in 20 mM HEPES, pH 7.5, concentrations of NaCl from 100 mM to 2 M and 1 mM EDTA. 0.1% of glutaraldehyde (Sigma) was added and the crosslinking reaction was stopped after 10 min with 100 mM Tris-HCl, pH 7.5, for 15 min at room temperature. Protein was precipitated with 5% TCA for 60 min on ice and subsequently pelleted by centrifugation. The pellets were resuspended in sample buffer, loaded on an SDS-PAGE and stained with Coomassie Brilliant Blue.

Crosslinking Experiments with TF-K46C-BPIA

TF-K46C (60 µM) was reduced with 60 µM TCEP (Tris-[2-carboxylethylphosphine] hydrochloride, Pierce) in 20 mM HEPES, pH 7.5, 50 mM NaCl, 1 mM EDTA, for 30 min at room temperature. Twohundred-fifty µM of photoinducible crosslinker BPIA (benzophenone-4-iodacetamide, Molecular Probes) was added and samples were incubated for 90 min at room temperature in the dark. To remove non-bound crosslinker the sample was dialyzed overnight against buffer.

For crosslinking studies, 2 µM of TF-K46C-BPIA and 8 µM of TF fragments were incubated for 30 min at 30 °C in the dark. To start the crosslinking reaction samples were subjected for 10 min to UV irradiation at 365 nm. Aliquots of the samples were analyzed by SDS-PAGE and the gel was silver-stained.

Binding of TF and TF-K46C-BPIA to Ribosomes

Ribosome binding analysis was performed according to Hesterkamp *et al.* (1997) with minor modifications. Two µM of ribosomes purified from TF-deficient cells were incubated with either increasing amounts of TF (0.5 to 20 µM) or 4 µM TF-K46C-BPIA for 30 min at 30 °C. Crosslinking was carried out as described above. Soluble TF was separated from ribosome bound species by sucrose cushion centrifugation and analyzed by SDS-PAGE (Schaffitzel *et al.*, 2001).

References

Bukau, B., Deuerling, E., Pfund, C. and Craig, E.A. (2000). Getting newly synthesized proteins into shape. Cell *101*, 119 – 122.

Deuerling, E., Schulze-Specking, A., Tomoyasu, T., Mogk, A. and Bukau, B. (1999). Trigger factor and DnaK cooperate in folding of newly synthesized proteins. Nature *400*, 693 – 696.

Hartl, F.U. and Hayer-Hartl, M. (2002). Molecular chaperones in the cytosol: from nascent chain to folded protein. Science *295*, 1852 – 1858.

Hesterkamp, T., Deuerling, E. and Bukau, B. (1997). The amino-terminal 118 amino acids of *Escherichia coli* trigger factor constitute a domain that is necessary and sufficient for binding to ribosomes. J. Biol. Chem. *272*, 21865 – 21871.

Hesterkamp, T., Hauser, S., Lütcke, H. and Bukau, B. (1996). *Escherichia coli* trigger factor is a prolyl isomerase that associates with nascent polypeptide chains. Proc. Natl. Acad. Sci. USA *93*, 4437 – 4441.

Kramer, G., Rauch, T., Rist, W., Vorderwülbecke, S., Patzelt, H., Schulze-Specking, A., Ban, N., Deuerling, E. and Bukau, B. (2002). The protein L23 functions as a chaperone docking site on the ribosome. Nature, in press.

Lill, R., Crooke, E., Guthrie, B. and Wickner, W. (1988). The 'Trigger factor cycle' includes ribosomes, presecretory proteins and the plasma membrane. Cell *54*, 1013 – 1018.

Patzelt, H., Rudiger, S., Brehmer, D., Kramer, G., Vorderwulbecke, S., Schaffitzel, E., Waitz, A., Hesterkamp, T., Dong, L., Schneider-Mergener, J., Bukau, B. and Deuerling, E. (2001). Binding specificity of *Escherichia coli* trigger factor. Proc. Natl. Acad. Sci. USA *98*, 14244 – 14249.

Ramm, K. and Pluckthun, A. (2001). High enzymatic activity and chaperone function are mechanistically related features of the dimeric *E. coli* peptidyl-prolyl-isomerase FkpA. J. Mol. Biol. *310*, 485 – 98.

Richter, K., Muschler, P., Hainzl, O. and Buchner, J. (2001). Coordinated ATP hydrolysis by the Hsp90 dimer. J. Biol. Chem. *276*, 33689 – 96.

Schaffitzel, E., Rüdiger, S., Bukau, B. and Deuerling, E. (2001). Functional dissection of trigger factor and DnaK: interactions with nascent polypeptides and thermally denatured proteins. Biol. Chem. *382*, 1235 – 1243.

Scholz, C., Stoller, G., Zarnt, T., Fischer, G. and Schmid, F.X. (1997). Cooperation of enzymatic and chaperone functions of trigger factor in the catalysis of protein folding. EMBO J. *16*, 54 – 58.

Scholz, C., Mücke, M., Rape, M., Pecht, A., Pahl, A., Bang, H. and Schmid, F.X. (1998). Recognition of protein substrates by the prolyl isomerase trigger factor is independent of proline residues. J. Mol. Biol. *277*, 723 – 732.

Schonfeld, H.J. and Behlke, J. (1998). Molecular chaperones and their interactions investigated by analytical ultracentrifugation and other methodologies. Methods Enzymol. *290*, 269 – 96.

Stoller, G., Ruecknagel, K.P., Nierhaus, K.H., Schmid, F.X., Fischer, G. and Rahfeld, J.-U. (1995). A ribosome-associated peptidyl-prolyl *cis/trans* isomerase identified as the trigger factor. EMBO J. *14*, 4939 – 4948.

Teter, S.A., Houry, W.A., Ang, D., Tradler, T., Rockabrand, D., Fischer, G., Blum, P., Georgopoulos, C. and Hartl, F.U. (1999). Polypeptide flux through bacterial Hsp70: DnaK cooperates with trigger factor in chaperoning nascent chains. Cell *97*, 755 – 765.

Valent, Q.A., Kendall, D.A., High, S., Kusters, R., Oudega, B. and Luirink, J. (1995). Early events in preprotein recognition in *E. coli*: interaction of SRP and trigger factor with nascent polypeptides. EMBO J. *14*, 5494 – 5505.

Wen, J., Arakawa, T. and Philo, J.S. (1996). Size-exclusion chromatography with on-line light-scattering, absorbance, and refractive index detectors for studying proteins and their interactions. Anal. Biochem. *240*, 155 – 66.

Zarnt, T., Tradler, T., Stoller, G., Scholz, C., Schmid, F.X. and Fischer, G. (1997). Modular structure of the trigger factor required for high activity in protein folding. J. Mol. Biol. *271*, 827 – 837.